01,10,19

Study of the FCC-Au properties in a wide range of temperatures and pressures

© M.N. Magomedov

Institute for geothermal problems and renewable energy —
branch of the joint Institute of high temperatures of the Russian Academy of Sciences,
Makhachkala, Russia

E-mail: mahmag4@mail.ru

Received March 21, 2022
Revised April 5, 2022
Accepted April 6, 2022

The properties of the FCC-of the gold crystal were calculated using an analytical method (without computer modeling) in the temperature range: $T = 10-1337$ K and pressures: $P = 0-110$ GPa. The following properties were calculated: state equation, Debye temperature, first and second Gruneisen parameters, elastic modulus (B_T), thermal expansion coefficient (α_p), isochoric (C_v) and isobaric (C_p) heat capacity, specific surface energy. Derivatives of these properties also have been calculated both by temperature along three isobars and by pressure along three isotherms. The obtained results showed good agreement with the other authors results. It was shown that there is a certain temperature T_B in which the product $\alpha_p B_T$ does not change during the crystal compression. At $T > T_B$, the $\alpha_p B_T$ function increases, and at $T < T_B$, it decreases with an increase in pressure. For FCC-Au has been received $T_B = 132$ K. It was shown that the isotherms of the baric derivative of elastic modulus $B'(P)$ intersect at the point: $P > 21.58$ GPa, and $B'(P) = 7.43$. At $P < 21.58$ GPa, the $C'_v(P)$ function increases, and at $P > 21.58$ GPa, it decreases with increasing temperature. It was shown that the isotherm of the baric derivative of the isochoric heat capacity $C'_v(P)$ has a minimum, and the isotherm of the baric derivative of the isobaric heat capacity $C'_p(P)$ has both a minimum and a maximum. Based on the obtained dependencies, some approximations, which are used to calculate the properties of the crystal under high $P-T$-conditions, have been analyzed.

Keywords: gold, pressure, elastic modulus, thermal expansion, heat capacity, Debye temperature, Gruneisen parameter, surface energy.

DOI: 10.21883/PSS.2022.07.54579.319

1. Introduction

When studying the properties of a crystal in the region of high temperatures (T) and pressures (P), it is most difficult to estimate the dependence of the thermal expansion coefficient ($\alpha_p = (\partial \ln V/\partial T)_P$) on $P-T$-arguments. Meanwhile, it is the function $\alpha_p(P, T)$ that determines both the change in pressure upon isochoric heating of the crystal and the change in entropy (S) upon isothermal change in the volume (V) of the crystal

$$\alpha_p B_T = \left(\frac{\partial P}{\partial T}\right)_V = \left(\frac{\partial S}{\partial V}\right)_T, \qquad (1)$$

where $B_T = -V(\partial P/\partial V)_T$ is isothermal modulus of elasticity.

The function $\alpha_p(P, T)$ also determines the dependence of the isobaric heat capacity of the crystal (C_p) on $P-T$-arguments, which is very important for applications. Therefore, in order to somehow estimate the functions α_p, $\alpha_p B_T$, and C_p under high $P-T$-conditions, several approximations were proposed, among which the Birch approximation. In 1952, Francis Birch in his article [1] suggested that for silicates and oxides at high temperatures the product $\alpha_p B_T$ is independent of pressure

$$\alpha_p B_T = \text{const}. \qquad (2)$$

In 1975 in the article [2] in an experimental study of inert gas crystals, it was found that at high temperatures ($T > \Theta$ — Debye temperature) the function $(\partial P/\partial T)_V$ is independent of temperature and volume. In [3], when studying alkali halide crystals, it was found that the product $\alpha_p B_T$ varies slightly with volume. In [4] it was shown that for many metals and ionic crystals the „product $\alpha_p B_T$ varies by less than a few per cent between the Debye and melting temperatures“. It was also pointed out in the article [5] that for many minerals at high temperatures the product $\alpha_p B_T$ does not depend on temperature.

Thus, despite its simplicity, approximation (2) has received wide recognition and is used to calculate properties not only for crystalline substances, but also for amorphous, liquid and nanostructured substances [6–12]. The approximation (2) is sometimes also called as αB rule [8]. At the same time, it must be remembered that the approximation (2) arose and is still used due to the fact that it is calculated within the framework of a single method (analytical or computer) of the function $B_T(P, T)$, $\alpha_p(P, T)$ and $C_p(P, T)$ is still extremely difficult even for a single-component crystal [13–15]. As for the derivatives of the functions $\alpha_p(P, T)$ and $C_p(P, T)$ with respect to pressure along the isotherm, there are no such estimates in the literature yet. The same is the case with the study of the

specific (per unit area) surface energy (σ) of a crystal and the derivatives of the σ function with respect to temperature along the isobar and pressure along the isotherm.

In this regard, three problems were solved in this article.

1. A relatively simple analytical method for calculating the thermodynamic properties of a single-component substance crystal is proposed.

2. Using this method, the properties of gold were calculated in a wide range of $P-T-V$-arguments.

3. On the basis of the dependences obtained, both the approximation (2) and a number of other approximations, which are used to estimate the crystal properties under high $P-T$-conditions, were studied.

In this case, the calculations of the properties in this article were carried out both for an isobaric increase in temperature (along three isobars) and for isothermal compression of the crystal (along three isotherms). Using gold as an example, it was analyzed — how applicable various approximations are in various $P-T-V$-conditions.

Gold was selected because it is low oxidizable, inert and ductile metal that does not experience polymorphic phase transitions. The thermoelastic properties of gold have been relatively well studied experimentally under various $P-T$-conditions. In addition, gold is the most commonly used pressure calibration standard in experiments under high $P-T$-conditions.

2. Calculation method for properties of a single-component substance crystal

To calculate the lattice properties of a single-component crystal, it is necessary to determine both the interaction potential of its atom pair and the calculation method based on this potential. Let us represent the pair interatomic interaction as four parametric Mie–Lennard-Jones potential, which has the following form [16, ch. 7]:

$$\varphi(r) = \frac{D}{(b-a)}\left[a\left(\frac{r_0}{r}\right)^b - b\left(\frac{r_0}{r}\right)^a\right], \qquad (3)$$

where D and r_0 are the depth and the coordinate of the potential minimum and $b > a > 1$ are numerical parameters.

Then, using the approximation of „the interaction of only nearest neighbors“ the Debye temperature as a function of the first coordination number and the distance between the centers of the nearest atoms can be determined from the expression [17]:

$$\Theta(k_n, c) = A_w(k_n, c)\xi\left[-1 + \left(1 + \frac{8D}{k_B A_w(k_n, c)\xi^2}\right)^{1/2}\right]. \qquad (4)$$

Here $k_B = 1.3807 \cdot 10^{-23}$ J/K is Boltzmann constant, k_n is first coordination number, $c = (6k_p v/\pi)^{1/3}$ is distance between centers of the nearest atoms, k_p is structure packing factor, $v = V/N$ is specific volume, V and N are volume and number of crystal atoms.

The A_w function arises due to taking into account the energy of „zero vibrations“ of atoms in a crystal and has the following form:

$$A_w(k_n, c) = K_R \frac{5k_n ab(b+1)}{144(b-a)}\left(\frac{r_0}{c}\right)^{b+2}, \qquad (5)$$

$$K_R = \frac{\hbar^2}{k_B r_0^2 m}, \quad \xi = \frac{9}{k_n},$$

where m is atomic mass, $\hbar = 1.0546 \cdot 10^{-34}$ J · s — Plank's constant.

If we apply the approximation of „the interaction of only nearest neighbors“ and use the Einstein model for the crystal vibrational spectrum, then for the specific (per atom) Helmholtz free energy of the crystal, we can adopt the expression [16,18]:

$$f_H(k_n, c, T) = \left(\frac{k_n}{2}\right)DU(R) + 3k_B\Theta_E(k_n, c) \times \left\{\frac{1}{2} + \left(\frac{T}{\Theta_E(k_n, c)}\right)\ln\left[1 - \exp\left(-\frac{\Theta_E(k_n, c)}{T}\right)\right]\right\}, \qquad (6)$$

where Θ_E is the Einstein temperature, which is related to the Debye temperature by the [16,18]: $\Theta = (4/3)\Theta_E$ ratio, $R = r_0/c$ is relative linear density of the crystal, $U(R)$ is potential energy function, which, in accordance with (3), is equal to

$$U(R) = \frac{aR^b - bR^a}{b-a}.$$

Based on the expression (6) for the state equation (P) and the isothermal modulus of elasticity (B_T) one can obtain [19]:

$$P = -\left(\frac{\partial f_H}{\partial v}\right)_T = \left[\frac{k_n}{6}DU'(R) + 3k_B\Theta_E\gamma E_w\left(\frac{\Theta_E}{T}\right)\right]\frac{1}{v}, \qquad (7)$$

$$B_T = -v\left(\frac{\partial P}{\partial v}\right)_T = P + \left[\frac{k_n}{18}DU''(R) + 3k_B\Theta_E\gamma(\gamma - q) \times E_w\left(\frac{\Theta_E}{T}\right) - 3k_B\gamma^2 T F_E\left(\frac{\Theta_E}{T}\right)\right]\frac{1}{v}. \qquad (8)$$

The following functions are introduced here:

$$E_w(y) = 0.5 + \frac{1}{[\exp(y) - 1]},$$

$$F_E(y) = \frac{y^2\exp(y)}{[\exp(y) - 1]^2},$$

$$U'(R) = R\left[\frac{\partial U(R)}{\partial R}\right] = \frac{ab(R^b - R^a)}{b-a},$$

$$U''(R) = R\left[\frac{\partial U'(R)}{\partial R}\right] = \frac{ab(R^b - R^a)}{b-a}. \qquad (9)$$

Table 1. Properties of FCC-Au at $P = 0$ and $T = 300\,\mathrm{K}$ (The data known from the literature are given in the bottom line)

Properties	V, cm^3/mol	Θ, K	γ	α_p, $10^{-6}\mathrm{K}^{-1}$	B_T, GPa	$B'(P) = (\partial B_T/\partial P)_T$
Calculation	10.1973	197.098	2.951	43.039	164.365	8.245
Literature data	10.2055 [14]	170 [25]	2.52−3.38 [25]	42.24 [31]	162.6−168.2 [14]	4.62 ± 0.1 [14]
		162−168 [30]	2.95−3.15 [30]	42.6 [32]	161.7−171.7 [25]	5.26−6 [25]
	10.215 [25]	162.5 [31]	2.96 [31]	42−42.8 [33]	166.5−166.9 [30]	6.05−6.35 [30]
	10.210 [31]	165−180 [32]	2.95−3.215 [32]	41.47 [34]	167−171 [32]	5.0−6.2 [32]
	10.207 [32]	171−190 [33]	2.888 [34]		173.5−180.9 [33]	6.2−9.65 [33]
	10.215 [34]	179−179.5 [34]			167 [34]	5.81−5.90 [34]

From formula (4) it is easy to find expressions for the first (γ) and second (q) Gruneisen parameters, which have the form

$$\gamma = -\left(\frac{\partial \ln \Theta}{\partial \ln v}\right)_T = \frac{b+2}{6(1+X_w)},$$

$$q = \left(\frac{\partial \ln \gamma}{\partial \ln v}\right)_T = \gamma \frac{X_w(1+2X_w)}{(1+X_w)}. \qquad (10)$$

Here, the function $X_w = A_w\xi/\Theta$ is introduced, which determines the role of quantum effects in calculating the Gruneisen parameters. Since the Debye temperature from (4) does not depend on temperature during isochoric heating, the isochoric and isobaric heat capacities can be determined in the form [16,18]:

$$C_v = 3Nk_\mathrm{B} F_E\left(\frac{\Theta_E}{T}\right),$$

$$C_p = C_v(1+\gamma\alpha_p T), \qquad (11)$$

where the isobaric thermal volume-expansion coefficient can be calculated from the Gruneisen equation

$$\alpha_p = \frac{1}{v}\left(\frac{\partial v}{\partial T}\right)_P = \gamma\frac{C_v}{VB_T} = \frac{\gamma C_v}{NB_T[\pi r_0^3/(6k_p)]}\left(\frac{v_0}{v}\right),$$

$$v_0 = \frac{\pi r_0^3}{6k_p}. \qquad (12)$$

The resulting expressions (4)−(12) enable to calculate the dependence of both the state equation and the specified properties on the normalized volume $v/v_0 = (c/r_0)^3 = R^{-3}$ and temperature for a single-component crystal with a given structure (i.e. for given values of k_n and k_p), if the parameters of the interatomic potential (3) are known. This method has been successfully applied in calculating the properties of various polymorphic modifications of iron [19,20], silicon and germanium [21], isotopically different diamonds [22], and also for binary alloys [23].

Note that expressions (4)−(12) do not take into account either vacancies or self-diffusion of atoms, because, as was shown in [24], their influence becomes negligible when the crystal is compressed. Here, as well as in [19–24], the contribution of the electronic subsystem to the thermodynamic parameters is not taken into account, because the potential (3) describes the pair interaction of electrically neutral atoms. In addition, as was shown in articles [25–28], the errors that arise in the lattice properties calculation due to the exclusion of the electronic subsystem from consideration are negligibly small. For example, as indicated in [25], for gold the contribution of the electronic subsystem to the pressure is 0.01 and 0.5 GPa at 1000 and 5000 K, respectively. This contribution is much smaller than the error in pressure measurements at these temperatures.

The question arises: how accurate will be the calculations using the relatively simple analytical expressions presented here (4)−(12)? The answer to this question in relation to gold is contained below.

3. Calculation results of gold properties

To calculate the crystal properties using formulas (4)−(12), gold (Au, $m(\mathrm{Au}) = 196.967$ a.m.u.) was taken, whose melting point at $P = 0$ is $T_m(P = 0) = 1337.58\,\mathrm{K}$. Gold has a face centered cubic (FCC) structure ($k_n = 12$, $k_p = 0.7405$) and does not experience polymorphic phase transitions.

The parameters of pair interatomic potential for FCC-Au (3) were determined in [29], and have the following values:

$$r_0 = 2.87 \cdot 10^{-10}\,\mathrm{m}, \quad D/k_\mathrm{B} = 7446.04\,\mathrm{K},$$

$$b = 15.75, \quad a = 2.79. \qquad (13)$$

Table 1 presents the properties of FCC-Au calculated using the potential parameters from (13) at $P = 0$ and $T = 300\,\mathrm{K}$. As can be seen in Table 1, the agreement between the calculated data and the experimental and theoretical estimates of other authors is quite good.

3.1. State equations

Figure 1, *a* shows the behavior of the thermal state equation of the FCC-Au, i.e. the isothermal dependences of the pressure (P, in GPa) on volume (V, in cm^3/mol) along three isotherms (bottom−up): 100, 300, 1337 K. Solid curve is an experimental isotherm $T = 300\,\mathrm{K}$ from [25]. Our calculations: for $T = 100\,\mathrm{K}$ — lower dashed curve, for $T = 300\,\mathrm{K}$ — middle dashed curve, for $T = 1337\,\mathrm{K}$ —

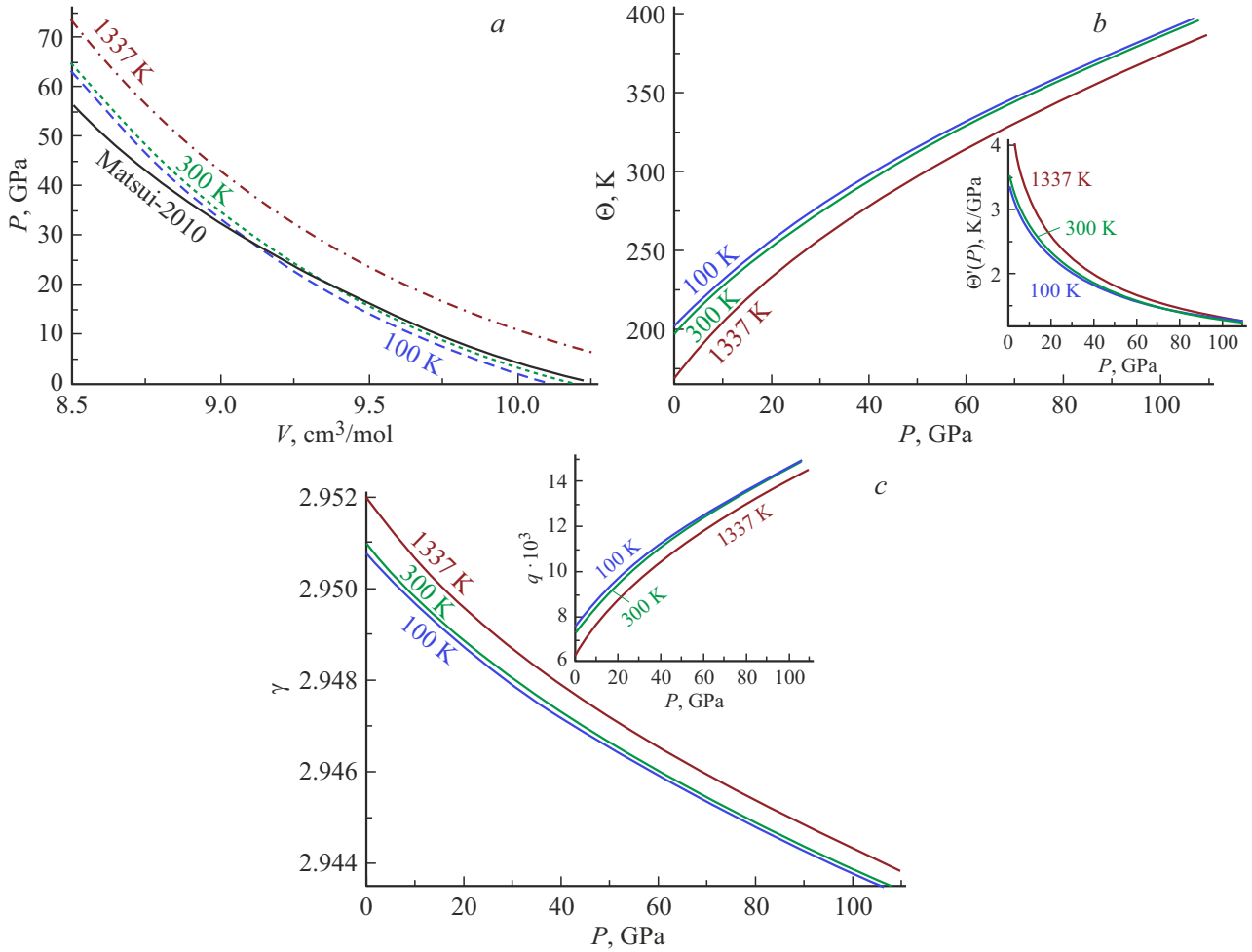

Figure 1. Isotherms of the state equation (a), Debye temperature (b), first (c) and second (on inset) Gruneisen parameters for FCC-Au.

upper dashed curve. As can be seen in Fig. 1, a, the agreement between the calculated dependence $P(V,\ 300\,\mathrm{K})$ and the experimental isotherm from [25] is quite good.

By calculating the dependence $P(V)$ and the dependence of some parameter $X(V)$ along a certain isotherm, one can obtain the pressure dependence of this parameter $X(P)$ along the same isotherm. Figure 1, b, c shows the baric dependences of the Debye temperature calculated in this way, the derivative of the Debye temperature with respect to pressure $(\Theta'(P) = (\partial\Theta/\partial P)_T$, in K/GPa), the first and second Gruneisen parameters for FCC-Au along isotherms 100, 300, 1337 K. It can be seen on these graphs that while the functions Θ, γ and q, do not have an explicit temperature dependence in expressions (4) and (10), with an isobaric increase in temperature, they change: the quantities Θ and q decrease, while $\Theta'(P)$ and γ increase.

As can be seen in formula (4), our method uses the approximation: $\Theta'(T) = (\partial\Theta/\partial T)_v = 0$, which is called „the Debye–Gruneisen quasi-harmonic approximation“ [35]. If this approximation is not used, then, as shown in [36], the formulas for the heat capacity and thermal expansion coefficient will include the first and second derivatives of the function $\Theta(T)$ with respect to temperature. This will significantly complicate the calculations, especially since the correct definition of the function $\Theta(T)$ is very difficult [36].

In many articles (for example, in [13,14,25,26,32]) the dependence of the Gruneisen parameter on volume is described by the expression

$$\gamma(V) = \gamma(V_0)\left(\frac{V}{V_0}\right)^q,$$

where it is assumed that the second Gruneisen parameter does not depend on V/V_0, i.e., on pressure: $q = \mathrm{const}$. As can be seen on the inset in Fig. 1, c the function $q(P)$ on the interval from 0 to 100 GPa almost doubles. It was shown in the articles [17,19,24] that the functions $\Theta(V)$ and $q(V)$ increase as the crystal is compressed, while the function $\gamma(V)$ decreases

$$\lim_{V/V_0\to 0}\Theta = \Theta_{\max} = \frac{4k_nD}{9k_\mathrm{B}}, \qquad \lim_{V/V_0\to 0}\gamma = \gamma_{\min} = 0,$$

$$\lim_{V/V_0\to 0} q = q_{\max} = \frac{b+2}{3}.$$

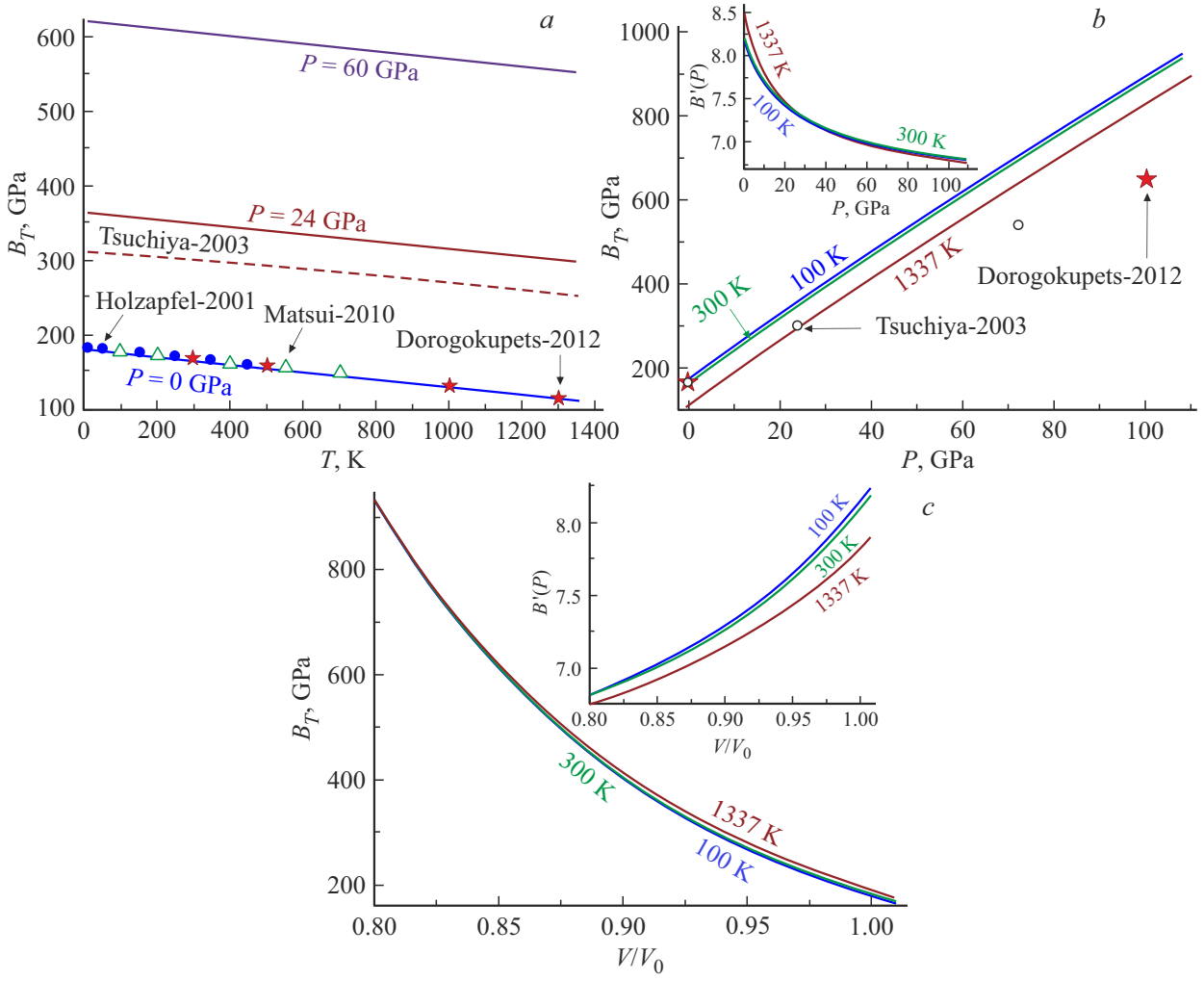

Figure 2. Dependence of the modulus of elasticity on temperature along three isobars (a), on pressure (b), and on normalized volume (c) along three isotherms for FCC-Au. The insets in Fig. 2, *d, c* show the dependence of the derivative of the modulus of elasticity with respect to pressure ($B'(P)$) on pressure (b) and on the normalized volume (c).

Thus, the assumption about the constancy of the value q is not correct.

3.2. Modulus of elasticity

Figure 2, *a* shows the change in the isothermal modulus of elasticity (B_T, in GPa) for FCC-Au with an isobaric change in temperature along three isobars (bottom–up): 0, 24, 60 GPa. Solid lines show our calculations. As can be seen, the calculated isobar dependence $B_T(T)$ at $P = 0$ (lower solid line) is in good agreement with the experimental dependences from the articles [25] (open triangles) and [30] (solid circles). The dashed line shows the theoretical isobar dependence $B_T(T)$ from [32] for $P = 24$ GPa. In the article [32] the gold properties were calculated based on the „first principles“ within „density-functional theory“ (DFT) using the local density approximation. The asterisks in Fig. 2, *a* show the results of calculations at $P = 0$ from [34], which were obtained „by simultaneously optimizing of shock-wave data, ultrasonic, X-ray, dilatometric and thermochemical measurements“.

Fig. 2, *b* shows the change in the B_T function for FCC-Au at an isothermal change in pressure, while Fig. 2, *c* — at isothermal change of normalized volume: $V/V_0 = v/v_0 = (c/r_0)^3 = R^{-3}$, where value v_0 is defined in (12). Using the value r_0 from (13) we get: $V_0 = v_0 N_A = 10.0663\,\text{cm}^3/\text{mol}$, where $N_A = 6.0221367 \cdot 10^{23}\,\text{mol}^{-1}$ is Avogadro constant. The symbols in Fig. 2, *b* show the theoretical results obtained for $T = 300$ K: open circles — from [32], solid asterisks — from [34]. The insets in Fig. 2, *b, c* show the dependences of the derivative of the modulus of elasticity with respect to pressure calculated along three isotherms ($B'(P) = (\partial B_T/\partial P)_T$) on pressure and on normalized volume, respectively. As can be seen, the isotherms of the function $B'(P)$ intersect at the point: $P = 21.58$ GPa, $B'(P) = 7.43$. At this pressure, the function $B'(P)$ does not depend on temperature.

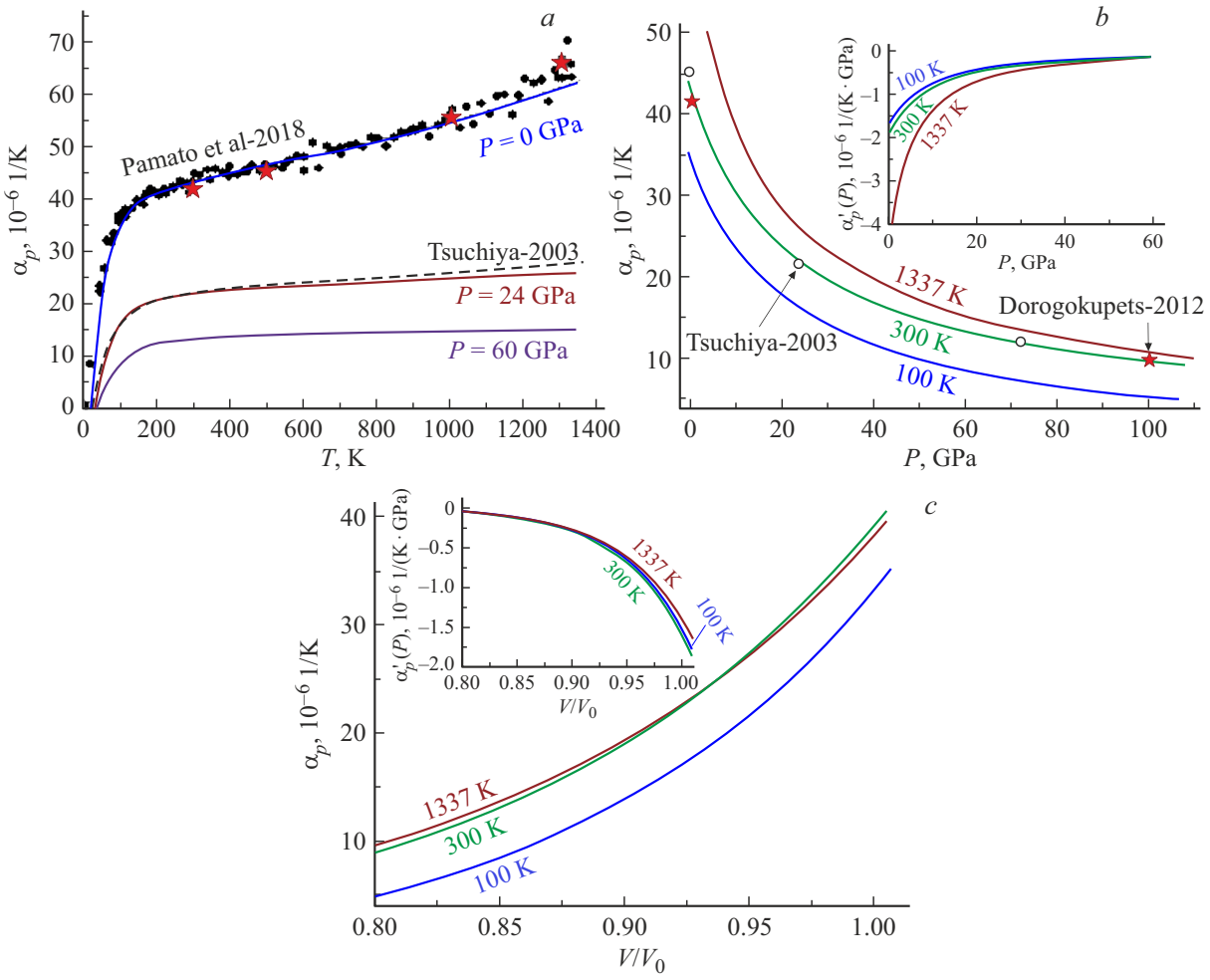

Figure 3. Dependence of the thermal expansion coefficient on temperature along three isobars (a), on pressure (b) and on normalized volume (c) along three isotherms. The insets in Fig. 3, b, c show the dependence of the derivative of the thermal expansion coefficient with respect to pressure ($\alpha'_p(P)$) on pressure (b) and normalized volume (c).

In 1944, F.D. Murnaghan in [37] proposed to calculate the baric dependence of the isothermal modulus of elasticity of solid matter at $T \gg \Theta$ by restricting with a linear dependence, i.e. using an approximation of the form

$$B_T(P) \equiv B_T(0) + \left(\frac{\partial B_T}{\partial P}\right)_{P=0} P = B_T(0) + B'(P)_0 P. \quad (14)$$

As it turned out later, the approximation (14), despite its simplicity, is satisfied well for many substances and, therefore, was called the „Murnaghan approximation“ [7] in the literature. As can be seen in Fig. 2, b, approximation (14) is satisfied quite well, but it must be borne in mind that with increasing temperature, the value of $B_T(0)$ decreases, and the value of $B'(P)_0$ increases. As for the isothermal dependence $B_T(V/V_0)$, then, as can be seen in Fig. 2, c, this dependence is non-linear.

3.3. Thermal expansion coefficient

Figure 3, a shows the change in the thermal expansion coefficient (α_p, in 10^{-6} 1/K) for FCC-Au at isobaric temperature change along three isobars (top–down): 0, 24, 60 GPa. Solid lines show our calculations. As can be seen, the calculated isobar dependence $\alpha_p(T)$ at $P = 0$ (upper solid line) is in good agreement with the experimental data from the article [33] (solid circles). Asterisks show the results of calculations for $P = 0$ from [34]. The dashed line, which merges with our solid line, shows the theoretical isobar dependence $\alpha_p(T)$ for $P = 24$ GPa from [32].

Figure 3, b shows the change in the α_p function for FCC-Au with an isothermal change in pressure $\alpha_p(P)$, while Figure 3, c — under an isothermal change in the normalized volume $\alpha_p(V/V_0)$. The isotherms 100, 300, 1337 K are shown bottom–up, respectively. The symbols in Fig. 3, b show the theoretical results obtained at $T = 300$ K: open circles — from [32], solid asterisks — from [34]. The insets in Fig. 3, b, c show the dependences of the derivative of the thermal expansion coefficient with respect to pres-

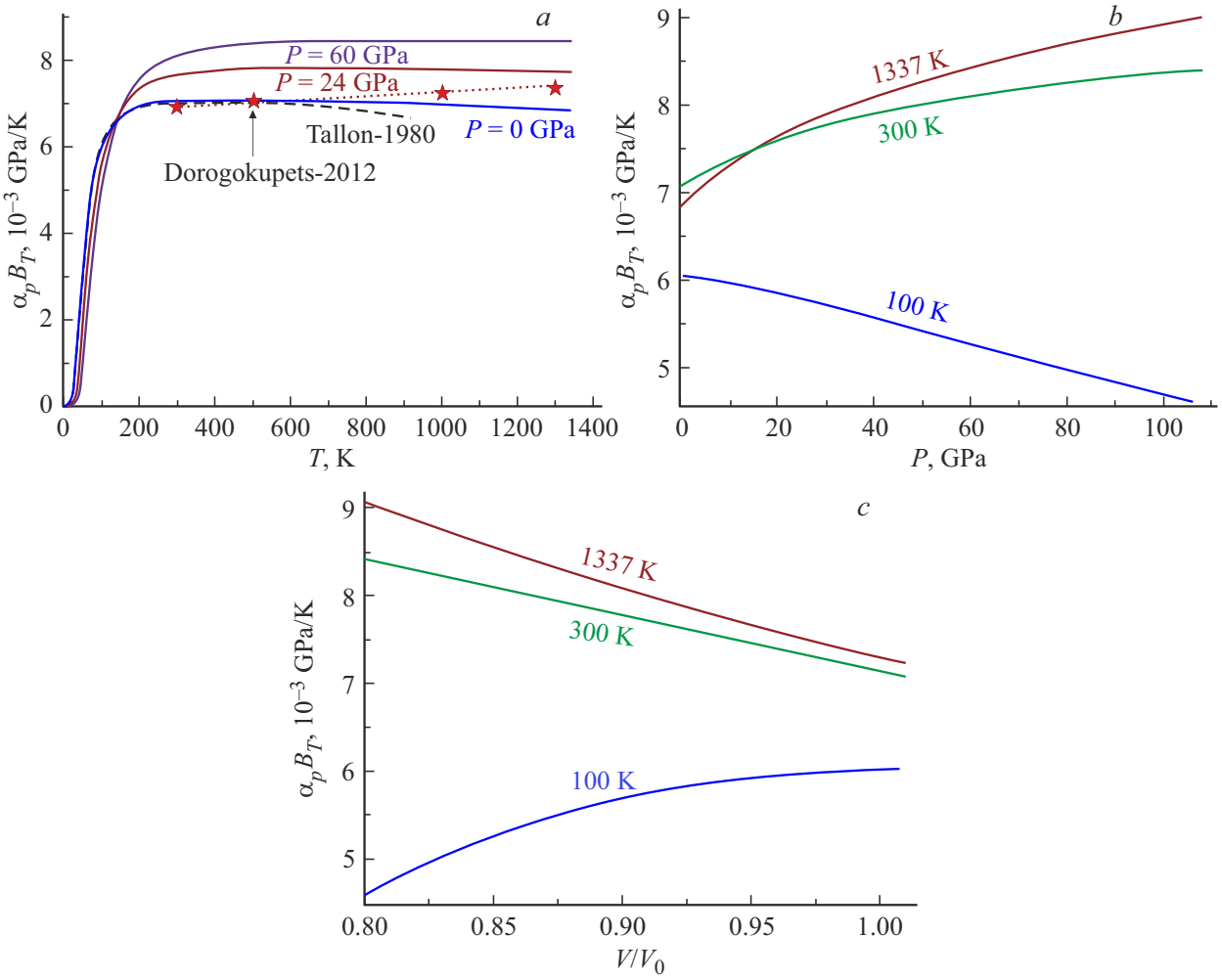

Figure 4. Dependence of the $\alpha_p B_T$ function on the temperature along three isobars (a), on the pressure (b), and on the normalized volume (c) along three isotherms

sure calculated along three isotherms ($\alpha'_p(P) = (\partial\alpha_p/\partial P)_T$, in $10^{-6}\,1/(\text{GPa}\cdot\text{K})$) on pressure and normalized volume respectively.

It follows from formulas (7)–(11) that under ultimate compression, i.e. at $V/V_0 \to 0$, the following is true: $P \to \infty$, $B_T V \to \infty$, $\gamma \to 0$ and $C_v \to \text{const}$. Then from (12) it is easy to obtain

$$\lim_{V/V_0 \to 0} \alpha_p = (\alpha_p)_{\min} = +0.$$

It can be seen in Fig. 3, *b* that the baric dependences $\alpha_p(P)$ are non-linear. As was shown in [19] using iron as an example, the isothermal dependence $\alpha_p(P)$ is well approximated by a second-order exponential decay function of the following type:

$$\alpha_p(P) = y_0 + A_1 \exp\left(-\frac{P}{t_1}\right) + A_2 \exp\left(-\frac{P}{t_2}\right), \qquad (15)$$

where the adjustable constants $y_0 \geq 0$, A_1, A_2, t_1, t_2 depend on the temperature.

Note that in some articles, to approximate the function $\alpha_p(P)$ or $\alpha_p(V/V_0)$, a finite power dependence is used

$$\alpha_p(P) = a_0 + \sum_{i=1}^{k} a_i \left(\frac{P}{P_0}\right)^i,$$

$$\alpha_p\left(\frac{V}{V_0}\right) = a'_0 + \sum_{i=1}^{k} a'_i \left(\frac{V}{V_0}\right)^i. \qquad (16)$$

Having determined the adjusting constants in (16) based on the experimental data in the low pressure region, the authors of the approximations (16) then extrapolate them to the high pressure region, i.e. to $P \to \infty$ or $V/V_0 \to 0$. In this way, they get that starting from a certain value P_x or $(V/V_0)_x$, the function α_p moves into the negative region. It is this result that was obtained in a number of articles (for example, in [38,39]). However, if approximation (15) is used, then this erroneous result will not be obtained.

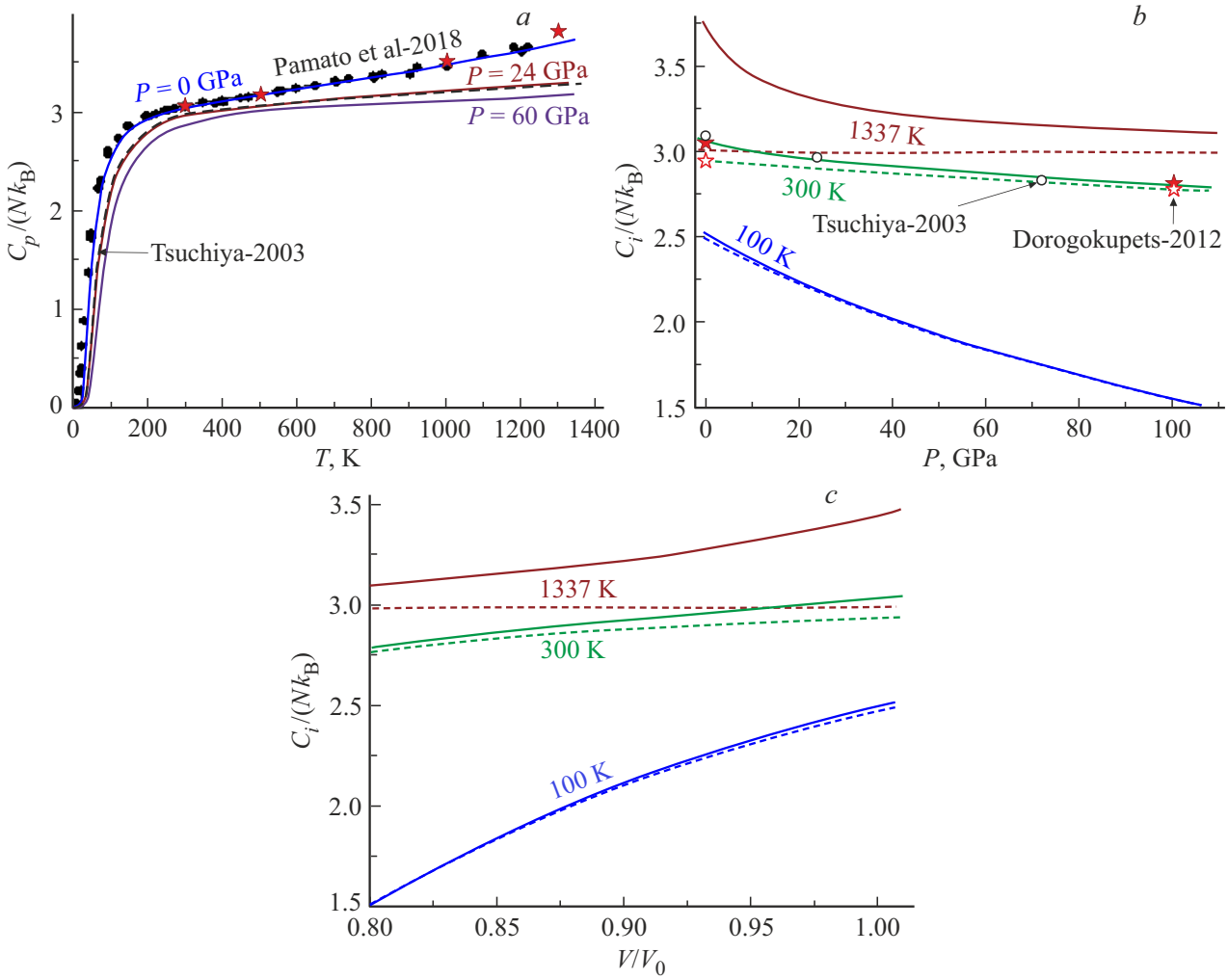

Figure 5. Dependence of normalized isobaric heat capacity on temperature along three isobars (a). Dependence of normalized isobaric (solid lines) and isochoric (dashed lines) heat capacity on pressure (b) and normalized volume (c) along three isotherms.

3.4. Product of $\alpha_p B_T$

Figure 4, a shows the temperature dependence of the function $\alpha_p B_T$ (in 10^{-3} GPa/K) for FCC-Au along three isobars (bottom–up): 0, 24, 60 GPa. Solid lines show our calculations. The dashed line and asterisks show the dependences obtained for $P = 0$ GPa in [4] and [34], respectively. Figure 4, b shows the change in the $\alpha_p B_T$ function for FCC-Au at an isothermal change in pressure, and Figure 4, c — at an isothermal change of the normalized volume. The isotherms 100, 300, 1337 K are shown bottom–up, respectively.

As can be seen on these plots, the isobar $\alpha_p B_T(T)$ has a maximum, which shifts towards higher temperatures with increasing pressure on the isobar. It can be seen in Fig. 4, b, c that the value of $\alpha_p B_T$ at $T > \Theta$ increases at an isothermal increase in pressure or at an isothermal decrease in the normalized volume. Therefore, in the general case, approximation (2) is not satisfied for isothermal crystal compression. At the same time, there is a certain temperature T_B, in the region of which the approximation (2) can be considered applicable. As can be seen in Fig. 4, a for FCC-Au the value $T_B = 132$ K is obtained.

3.5. Isochoric and isobaric heat capacity

Figure 5, a shows the change in the normalized isobaric heat capacity for FCC-Au as the temperature changes along three isobars (top–down): 0, 24, 60 GPa. Solid lines show our calculations. Solid circles show experimental data for $P = 0$ from [33]. The asterisks show the results for $P = 0$ from [34]. The dashed line merging with our solid line is the theoretical dependence obtained at $P = 24$ GPa in [32].

Figure 5, b shows the change in the normalized isobaric (solid lines) and isochoric (dashed lines) heat capacity for FCC-Au at an isothermal change in pressure, and Figure 5, c — at an isothermal change in the normalized volume. The isotherms 100, 300, 1337 K are shown bottom–up, respectively. The symbols in Fig. 5, b show

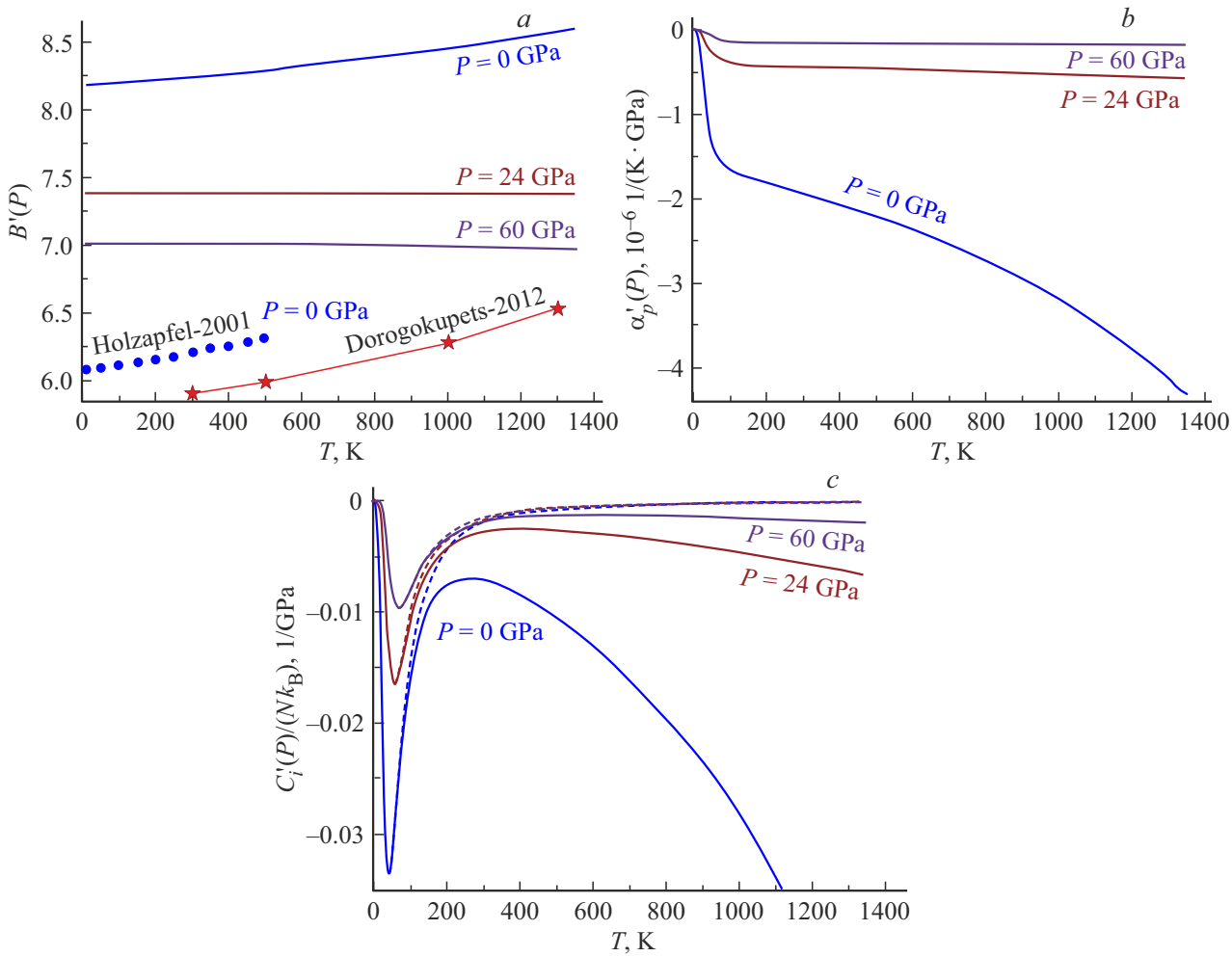

Figure 6. Temperature dependences of the baric derivatives of the modulus of elasticity (a), thermal expansion coefficient (b) and normalized isobaric ($i = p$, solid lines) and isochoric ($i = v$, dashed lines) heat capacities (c) for FCC-Au along isobars 0, 24, 60 GPa.

the theoretical results obtained for $T = 300$ K: circles — from [32], asterisks — from [34].

In some articles, when studying the dependence of the crystal heat capacity on $P-T$-arguments at $T > \Theta$, approximations are used that follow from the Dulong–Petit law (Dulong–Petit law):

$$C_p \cong C_v = 3Nk_B, \quad \left(\frac{\partial C_p}{\partial T}\right)_P \equiv \left(\frac{\partial C_v}{\partial T}\right)_P = 0,$$

$$\left(\frac{\partial C_p}{\partial P}\right)_{T>\Theta} \equiv \left(\frac{\partial C_v}{\partial P}\right)_{T>\Theta} = 0,$$

$$\left(\frac{\partial C_p}{\partial (V/V_0)}\right)_{T>\Theta} \equiv \left(\frac{\partial C_v}{\partial (V/V_0)}\right)_{T>\Theta} = 0. \qquad (17)$$

It can be seen in Fig. 5 that the approximations from (17) can lead to noticeable errors.

At ultimate compression i.e. at $V/V_0 \to 0$, the Debye temperature increases and the following relations are fulfilled: $\Theta \to \Theta_{\max}$ and $C_p \to C_v$. In this case, if the Dulong–Petit law was satisfied at low pressures, and the condition $T < \Theta(P)$ begins to be satisfied upon compression, then the heat capacity becomes less than $3Nk_B$. In this case, the baric derivatives will already be different from zero.

At ultimate compression, if $T < \Theta_{\max}$, it is possible to reach the value: $C_p = C_v \cong +0$. Based on the parameters of the potential (13), for fcc-Au we get

$$\lim_{V/V_0 \to 0} \Theta = \Theta_{\max} = \frac{4k_n D}{9k_B} = 39721 \text{ K}.$$

However, all these considerations are valid if, when a crystal is compressed, its crystal structure and parameters of the interatomic potential do not change, i.e. the structure of the atom is preserved.

3.6. Baric derivatives

Figure 6 shows the temperature dependences of the baric derivatives of the following functions: modulus of elasticity ($B'(P) = (\partial B_T/\partial P)_T$ — Fig. 6, a), thermal expansion coefficient ($\alpha'_p(P) = (\partial \alpha_p/\partial P)_T$ — Fig. 6, b, in 10^{-6} 1/(GPa · K)), normalized isobaric ($i = p$, solid

lines) and isochoric ($i = v$, dashed lines) heat capacity $(C'_i(P)/(Nk_B)=(Nk_B)^{-1}(\partial C_i/\partial P)_T$ — Fig. 6, *c*, in GPa^{-1}). The calculations are performed along three isobars: 0, 24, 60 GPa. In Fig. 6, *a* the symbols show the results for $P = 0$ GPa from [30] (circles) and from [34] (asterisks).

As can be seen in Fig. 6, *a* and on the inset in Fig. 2, *b*, the function $B'(P)$ at $P < 21.58$ GPa increases linearly, and at $P > 21.58$ GPa the function $B'(P)$ slightly decreases with an isobaric increase in temperature. In the region $17 < P < 27$ GPa, the function $B'(P)$ is practically independent of temperature during isobaric heating.

It can be seen in Fig. 6, *a, c* that the function $\alpha'_p(P)$ weakly depends on temperature at $T > 150$ K and $P > 24$ GPa. The functions $C'_v(P)$ and $C'_p(P)$ have minima, which are located at the points

T=41 K and $C'_i(P)/(Nk_B)=-0.0335\,GPa^{-1}$ for P=0 GPa,

T=59 K and $C'_i(P)/(Nk_B)=-0.0166\,GPa^{-1}$ for P=24 GPa,

T=70 K and $C'_i(P)/(Nk_B)=-0.0097\,GPa^{-1}$ for P=60 GPa.

The function $C'_p(P)$ have maximum, which is located at the point

T=265 K and $C'_p(P)/(Nk_B)=-0.007\,GPa^{-1}$ for P=0 GPa,

T=421 K and $C'_p(P)/(Nk_B)=-0.0025\,GPa^{-1}$ for P=24 GPa,

T=602 K and $C'_p(P)/(Nk_B)=-0.0012\,GPa^{-1}$ for P=60 GPa.

4. Calculation of the surface energy of gold

The value of the specific (per unit area) surface energy (σ) of a crystal is one of the most important parameters that determine its strength and adhesion properties. In this regard, several different methods for calculating the σ value for a single-component substance crystal have been proposed to date (e.g. see[40–50]). But most of these methods (e.g. [40,41,43,45,46,48,49]) work only at $T = 0$ K and $P = 0$. Therefore, the issue of the dependence of the value σ on the $P-T$-conditions in which the crystal is located is topical.

In articles [42,44,47,50] various methods for calculating the derivative of the σ function with respect to temperature were proposed: $\sigma'(T) = (\partial\sigma/\partial T)$. But, due to the absence of the state equation for the studied substances in these articles, it remains unclear — whether the expression for $\sigma'(T)$ proposed in these articles is isochoric $(\sigma'(T)_v)$ or isobaric $(\sigma'(T)_P)$ derivative?

As for the surface energy dependence on pressure, there are no expressions for calculating the function $\sigma'(P) = (\partial\sigma/\partial P)_T$ in the literature yet, and therefore no one has estimated this value. The problem here is related to the fact that in the theoretical models within which the function σ was calculated, the state equation of the crystal taking into account the surface was not obtained. Meanwhile, the dependence $\sigma(P)$ is necessary for studying both the initiation of a crack under pressure action on a macrocrystal and for obtaining the state equation for a nanocrystal.

To calculate the surface properties of both macro- and nanocrystals, we developed the RP-model [51], which uses the potential of pair interatomic interaction (3). Within the framework of the RP-model, for the specific surface energy of the face (100) of a macrocrystal (σ), its isochoric and isobaric derivatives with respect to temperature, the following expressions [51] were obtained:

$$\sigma = -\frac{k_n D R^2}{12\alpha^{2/3} r_0^2}\,[U(R) + 3H_w(R, T)], \tag{18}$$

$$\sigma'(T)_v = \left(\frac{\partial\sigma}{\partial T}\right)_v = -\frac{3k_B R^2\gamma}{2\alpha^{2/3}(b+2)r_0^2}\,F_E\left(\frac{\Theta_E}{T}\right), \tag{19}$$

$$\sigma'(T)_P = \left(\frac{\partial\sigma}{\partial T}\right)_P = \sigma'(T)_v + v\alpha_P\left(\frac{\partial\sigma}{\partial v}\right)_T$$

$$= \sigma'(T)_v - \frac{2}{3}\,\sigma\alpha_P\Delta_P. \tag{20}$$

The functions introduced here have the following form: $\alpha = \pi/(6k_p)$,

$$H_w(R, T) = \frac{6\gamma}{(b+2)}\,\frac{k_B\Theta_E}{Dk_n}\,E_w\left(\frac{\Theta_E}{T}\right),$$

$$\Delta_P = -\frac{1}{2}\left[\frac{\partial\ln(\sigma)}{\partial\ln(c)}\right]_T = -\frac{3}{2}\left[\frac{\partial\ln(\sigma)}{\partial\ln(V/V_0)}\right]_T$$

$$= 1 + \frac{U'(R) - \left[q - \gamma t_y\left(\frac{\Theta_E}{T}\right)\right]9H_w(R, T)}{2[U(R) + 3H_w(R, T)]}, \tag{21}$$

$$t_y(y) = 1 - \frac{2y\exp(y)}{[\exp(2y) - 1]}.$$

At $T \to 0$ K, the functions from (19) and (20) tend to zero for any value R, which agrees with the third law of thermodynamics in Planck's „strong" formulation.

Table 2 shows the results of calculations using formulas (18)–(21) and potential parameters from (13) of surface properties of FCC-Au at $P = 0$ and at three temperatures: T = 100, 300, 1337 K. The bottom line shows experimental and theoretical data known from the literature (in parentheses). As can be seen, the agreement between our calculations and experimental data is quite good.

Figure 7, *a* shows the calculated baric dependences of the specific surface energy (in 10^{-3} J/m^2) of the face (100) for FCC-Au along isotherms (top–down) 100, 300, 1337 K. It can be seen that at a certain pressure the function $\sigma(P)$ reaches its maximum with the following coordinates:

$\sigma = 1.628$ J/m^2 and $P = 27$ GPa for $T = 100$ K,

$\sigma = 1.613$ J/m^2 and $P = 28.6$ GPa for $T = 300$ K,

$\sigma = 1.555$ J/m^2 and $P = 36$ GPa for $T = 1337$ K.

Table 2. Values of surface properties calculated for FCC-Au at $P = 0$ for three temperatures. (The bottom line shows experimental and theoretical (in brackets) data of other authors)

T, K	v/v_0	$\sigma(100)$, 10^{-3} J/m^2	$-\sigma'(T)_v$, mkJ/(m^{2}K)	$-\sigma'(T)_p$, mkJ/(m^{2}K)	$\sigma'(P)_T$, mJ/(m^{2}GPa)	Δ_p
100	1.00487	1561.19	43.52	80.53	6.13	1.0299
300	1.01302	1542.47	51.17	99.43	6.82	1.0903
1337	1.06874	1422.80	50.37	133.85	12.20	1.4207
Experimental and (theoretical) data		1500–1506 [40], (1627) [40], 1500–1510 [41], (1630–1800) [41], 1500 [42,43], (1542) [42], (864–1627) [43], 1510 ± 160 [48], (850–1710) [48], 1500–1540 (0 K), 1333 (T_m) [52], 1410 ± 37 [53], 1363 [54] (1530 (300 K) – 1420 (1337 K)) [55]		125–156 [52] 500 [54] (92) [56]		

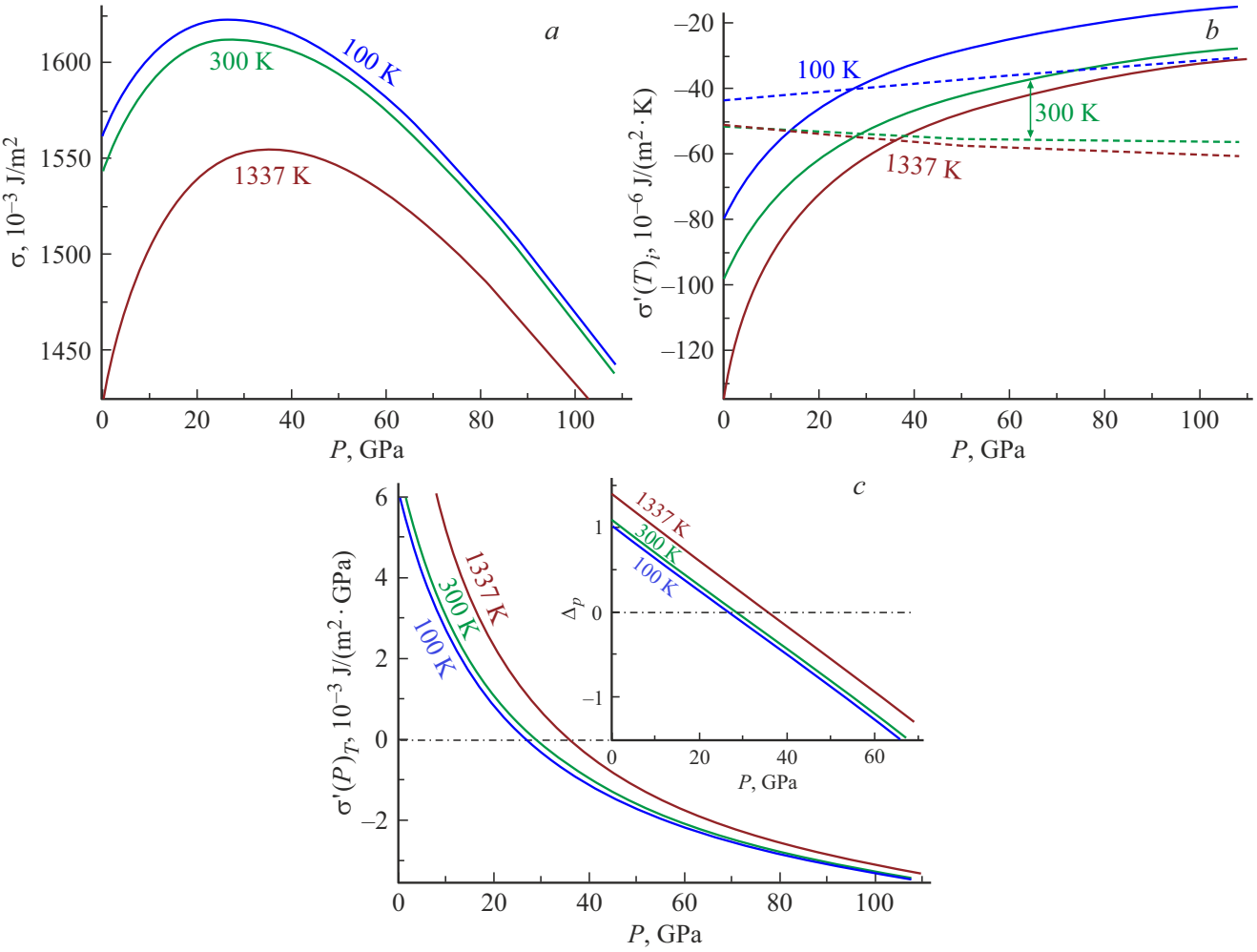

Figure 7. Baric dependence of the specific surface energy (a), its temperature derivative (b), and its pressure derivative (c) for FCC-Au along isotherms 100, 300, 1337 K.

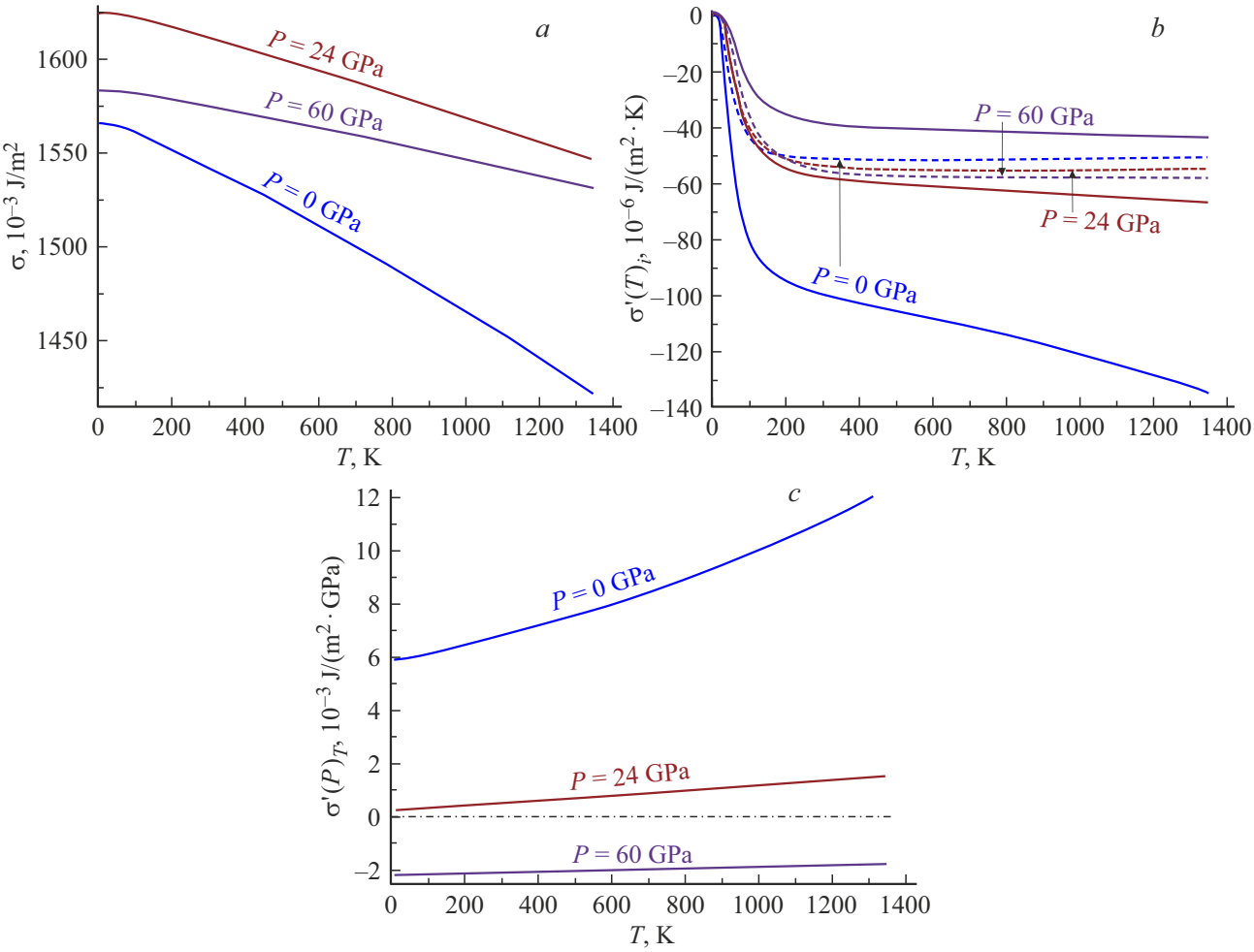

Figure 8. Temperature dependence of the specific surface energy (a), its temperature derivative (b), and its pressure derivative (c) for FCC-Au along isobars 0, 24, 60 GPa

Figure 7, b shows the calculated pressure dependences of the derivative of the specific surface energy of the face (100) with respect to temperature (in 10^{-6} J/(m $^2 \cdot$ K)) along isotherms (top−down) 100, 300, 1337 K. Solid lines are isobaric derivative, dashed lines are isochoric derivative. It can be seen that at low pressures (i.e. at $P < 27$ GPa for $T = 100$ K, at $P < 28.5$ GPa for $T = 300$ K, at $P < 36$ GPa for $T = 1337$ K) the following inequality is satisfied

$$|\sigma'(T)_P| > |\sigma'(T)_v|.$$

However, at high pressures, this inequality is reversed. Therefore, for a crystal, it is impossible to equate the isochoric and isobaric derivatives of the σ function with respect to temperature, as is done in some articles.

Figure 7, c shows the calculated baric dependence of the derivative of the specific surface energy with respect to pressure (in 10^{-3} J/(m$^2 \cdot$ GPa)) for FCC-Au along isotherms (bottom−up) 100, 300, 1337 K. It can be seen that at the maximum point of the function $\sigma(P)$, its derivative $\sigma'(P)$ moves into the negative region of values. The inset shows the baric dependence of the function Δ_p from (21) along three isotherms (bottom−up): 100, 300, 1337 K. As can be seen, the function $\Delta_p(P)$ decreases linearly with increasing pressure, and at the maximum point of the function $\sigma(P)$, the function $\Delta_p(P)$ moves into the negative region of values.

Figure 8, a shows the temperature dependences of the specific surface energy (in 10^{-3} J/m^2) of the face (100) for FCC-Au along isobars 0, 24, 60 GPa. The dependence for the 60 GPa isobar lies between the dependences of the 0 and 24 GPa isobars. This is due to the fact that, as can be seen in Fig. 7, a, the pressure 60 GPa is located after the maximum of the $\sigma(P)$ function.

Figure 8, b shows the temperature dependences of the derivative of the specific surface energy with respect to temperature (in 10^{-6} J/(m$^2 \cdot$ K)) for FCC-Au along isobars (bottom−up) 0, 24, 60 GPa. Solid lines show isobaric derivatives: $\sigma'(T)_P$, dashed lines show isochoric derivatives: $\sigma'(T)_v$. It can be seen that with an isobaric increase in temperature, the value of σ decreases at any pressure. Therefore, in some articles, for the isobaric or isochoric temperature dependence of the specific surface energy, a linear approximation of the following form was

used [42,47,50,57]:

$$\sigma(T) = \sigma(T = 0\,\mathrm{K}) + \left(\frac{\partial\sigma}{\partial T}\right)_{i,T=0\,\mathrm{K}} T$$

$$= \sigma(0) + \sigma'(T)_{i,T=0\,\mathrm{K}}\, T. \qquad (22)$$

However, as can be seen in Fig. 8, approximation (22) is valid only at high temperatures and pressures. The use of the approximation (22) at low temperatures can lead both to quantitative errors and to violation of the third law of thermodynamics. This is due to the fact that the contribution of the surface to the specific (per atom) entropy and heat capacity (both isochoric: $i = v$, and isobaric: $i = p$) of the system is determined precisely by the function $\sigma'(T)_v$, i.e. the derivative of the specific surface energy with respect to temperature [58]:

$$s_{\mathrm{surf}} = -\left(\frac{\Sigma}{N}\right)\left(\frac{\partial\sigma}{\partial T}\right)_{v,N},$$

$$\left(\frac{C_i}{N}\right)_{\mathrm{surf}} = T\left(\frac{\partial s_{\mathrm{surf}}}{\partial T}\right)_{i,N} = -\left(\frac{\Sigma}{N}\right)T\left[\frac{\partial}{\partial T}\left(\frac{\partial\sigma}{\partial T}\right)_{v,N}\right]_{i,N}.$$

Here Σ is the surface area of the system.

At $T = 0\,\mathrm{K}$, according to the third law of thermodynamics in Planck's „strong" formulation, for the specific entropy (s), heat capacity, and function $\alpha_p B_T$ the following conditions must be satisfied:

$$\lim_{T\to 0\,\mathrm{K}} s = +0, \quad \lim_{T\to 0\,\mathrm{K}} \frac{C_i}{N} = +0, \quad \lim_{T\to 0\,\mathrm{K}} \alpha_p B_T = +0.$$

In this regard, as was shown in [58], the function σ must satisfy the following conditions:

$$\lim_{T\to 0\,\mathrm{K}}\left(\frac{\partial\sigma}{\partial T}\right)_{i,N} = -0, \quad \lim_{T\to 0\,\mathrm{K}}\left[\frac{\partial(\partial\sigma/\partial T)_{v,N}}{\partial v}\right]_{T,N} = -0,$$

$$\lim_{T\to 0\,\mathrm{K}} T\left[\frac{\partial}{\partial T}\left(\frac{\partial\sigma}{\partial T}\right)_{v,N}\right]_{i,N} = -0. \qquad (23)$$

Conditions (23) are valid for any crystal structure, at any specific volume and pressure, and also at any size and shape of a nanocrystal. Therefore, the use of the approximation (22) is not correct for extrapolating the $\sigma(T)$ function to the region of low temperatures.

Figure 8, *c* shows the calculated temperature dependence of the derivative of the specific surface energy with respect to pressure ($\sigma'(P)_T$, in $10^{-3}\,\mathrm{J/(m^2\cdot GPa)}$) for FCC-Au along isobars (top−down) 0, 24, 60 GPa. As can be seen, at $P > 24\,\mathrm{GPa}$ the function $\sigma'(P)_T$ changes linearly with increasing temperature.

Note that earlier in the article [55], this method was used to calculate the state equation and baric dependences of the properties of FCC-Au along the isotherms 300 and 1337 K. However, as it was shown in [59], the parameters of the interatomic potential (3) that were used in [55] provide smaller values of the modulus of elasticity and the Gruneisen parameter than the experimental ones. Therefore, further, in [29] and in this article, more correct parameters of the potential from (13) were used.

5. Conclusions

1. An analytical method is proposed that uses three adjustable parameters in the pair potential of the Mie–Lennard-Jones (3) interatomic interaction. The method was tested on FCC-Au, and it was shown that the method enables to calculate all crystal thermodynamic properties both along an isotherm and along an isobar or isochore.

2. Using this method, the state equation and properties of gold are calculated in the temperature range: $T = 10-1337\,\mathrm{K}$ and pressure: $P = 0-110\,\mathrm{GPa}$. Both temperature dependences of properties along three isobars and pressure dependences of properties along three isotherms are obtained. The results obtained showed good agreement with the experimental and theoretical data of other authors.

3. It is shown that there exists a certain temperature T_B at which the product $\alpha_p B_T$ does not change under isothermal compression of the crystal. I.e. in the region T_B approximation (2) can be considered applicable. At $T > T_B$ the function $\alpha_p B_T$ increases, and at $T < T_B$ the function $\alpha_p B_T$ decreases with an isothermal increase in pressure. For gold, $T_B = 132\,\mathrm{K}$ is obtained. It is shown that the isobar $\alpha_p B_T(T)$ has a maximum, which shifts towards higher temperatures with increasing pressure on the isobar.

4. For the first time, the baric derivatives of the Debye temperature, modulus of elasticity, thermal expansion coefficient, isochoric and isobaric heat capacity, and specific surface energy are calculated. It is shown that the isotherms of the function $B'(P)$ intersect at the point: $P = 21.58\,\mathrm{GPa}$, $B'(P) = 7.43$. The function $B'(P)$ at $P < 21.58\,\mathrm{GPa}$ increases linearly, and at $P > 21.58\,\mathrm{GPa}$ the function $B'(P)$ slightly decreases with an isobaric increase in temperature. In the region $17 < P < 27\,\mathrm{GPa}$, the function $B'(P)$ is practically independent of temperature during isobaric heating. It is shown that the $C'_v(P)$ isotherm has a minimum, while the $C'_p(P)$ isotherm has both a minimum and a maximum.

5. Calculations of the baric dependence of the specific surface energy showed that the function $\sigma(P)$ has a maximum, the position of which shifts towards higher pressures with increasing temperature. The isochoric and isobaric derivatives of the specific surface energy with respect to temperature are calculated for the first time. It is shown that the inequality $|\sigma'(T)_P| > |\sigma'(T)_v|$ is satisfied at low pressures. But at high pressures, this inequality is reversed.

6. Based on the dependences obtained, the applicability of approximations (2), (14), (16), (17) and (22), which are used to calculate the crystal properties under various $P-T$-conditions, is analyzed. It is pointed out that the second Gruneisen parameter cannot be considered a constant independent of pressure.

7. It is shown that approximation (22) is applicable only at high temperatures and pressures. The use of the approximation (22) at low temperatures can lead both to quantitative errors and to violation of the third law of thermodynamics.

We studied FCC-Au in [60]. In this article, the following parameters were calculated: Gibbs energy, enthalpy, entropy, and volume, both for the process of electrically neutral vacancies formation and for the atom self-diffusion process.

Acknowledgments

The author would like to thank S.P. Kramynin, K.N. Magomedov, Z.M. Surkhayeva and M.M. Gadzhieva for fruitful discussions and assistance in work.

Conflict of interest

The author declares that he has no conflict of interest.

References

[1] F. Birch. J. Geophys. Res. **57**, *2*, 227 (1952). DOI: 10.1029/JZ057i002p00227
[2] M.S. Anderson, C.A. Swenson. J. Phys. Chem. Solids **36**, *2*, 145 (1975). DOI: 10.1016/0022-3697(75)90004-9
[3] T. Yagi. J. Phys. Chem. Solids **39**, *5*, 563 (1978). DOI: 10.1016/0022-3697(78)90037-9
[4] J.L. Tallon. J. Phys. Chem. Solids **41**, *8*, 837 (1980). DOI: 10.1016/0022-3697(80)90028-1
[5] O.L. Anderson. Phys. Earth Planetary Interiors **22**, *3–4*, 165 (1980). DOI: 10.1016/0031-9201(80)90029-1
[6] O.L. Anderson, K. Zou. Phys. Chem. Minerals **16**, *7*, 642 (1989). DOI: 10.1007/BF00223312
[7] J. Shanker, M. Kumar. Phys. Status Solidi B **179**, *2*, 351 (1993). DOI: 10.1002/pssb.2221790209
[8] J. Rault. Eur. Phys. J. B **92**, *1*, 1 (2019). DOI: 10.1140/epjb/e2018-90452-6
[9] K. Kholiya, K. Pandey. J. Taibah Univer. Sci. **13**, *1*, 592 (2019). DOI: 10.1080/16583655.2019.1611369
[10] M. Goyal, B.R.K. Gupta. Mod. Phys. Lett. B **33**, *26*, 19503101 (2019). DOI: 10.1142/s021798491950310X
[11] M. Goyal. Chin. J. Phys. **66**, 453 (2020). DOI: 10.1016/j.cjph.2020.05.002
[12] R.L. Jaiswal, B.K. Pandey, D. Mishra, H. Fatma. Int. J. Thermodynam. **24**, *1*, 1 (2021). DOI: 10.5541/ijot.869865
[13] X. Qi, N. Cai, S. Wang, B. Li. J. Appl. Phys. **128**, *10*, 105105 (2020). DOI: 10.1063/5.0022536
[14] D. Ikuta, E. Ohtani, H. Fukui, T. Sakamaki, D. Ishikawa, A.Q. Baron. Large density deficit of Earth's core revealed by a multi-megabar primary pressure scale. arXiv preprint 2021. arXiv:2104.02076. https://arxiv.org/ftp/arxiv/papers/2104/2104.02076.pdf
[15] C. Malica, A. Dal Corso. J. Phys.: Condens. Matter **33**, *47*, 475901 (2021). DOI: 10.1088/1361-648X/ac2041
[16] E.A. Moelwyn-Hughes. Physical Chemistry. Pergamon Press, London (1961). 1333 p.
[17] M.N. Magomedov. Techn. Phys. **58**, *9*, 1297 (2013). DOI: 10.1134/S106378421309020X
[18] L.A. Girifalco. Statistical Physics of Materials. Wiley and Sons Ltd., N.Y. (1973). 346 p.
[19] M.N. Magomedov. Techn. Phys. **60**, *11*, 1619 (2015). DOI: 10.1134/S1063784215110195
[20] M.N. Magomedov. Techn. Phys. **65**, *10*, 1659 (2020). DOI: 10.1134/S1063784220100138
[21] M.N. Magomedov. Phys. Solid State **59**, *6*, 1085 (2017). DOI: 10.1134/S1063783417060142
[22] M.N. Magomedov. Techn. Phys. **64**, *6*, 834 (2019). DOI: 10.1134/S1063784219060100.
[23] M.N. Magomedov. Phys. Solid State **62**, *12*, 2280 (2020). DOI: 10.1134/S1063783420120197
[24] M.N. Magomedov. Phys. Met. Metallography **114**, *3*, 207 (2013). DOI: 10.1134/S0031918X13030113
[25] M. Matsui. J. Phys.: Conf. Ser. IOP Publ. **215**, *1*, 012197 (2010). DOI: 10.1088/1742-6596/215/1/012197
[26] X. Huang, F. Li, Q. Zhou, Y. Meng, K.D. Litasov, X. Wang, B. Liu, T. Cui. Sci. Rep. **6**, 19923 (2016). DOI: 10.1038/srep19923
[27] A.M. Molodets, A.A. Golyshev, D.V. Shakhrai. J. Exp. Theor. Phys. **124**, *3*, 469 (2017). DOI: 10.1134/S1063776117030049
[28] D.K. Belashchenko. Phys.−Uspekhi **63**, *12*, 1161 (2020). DOI: 10.3367/UFNe.2020.01.038761
[29] M.N. Magomedov. Phys. Solid State **63**, *9*, 1595 (2021). DOI: 10.1134/S1063783421090250
[30] W.B. Holzapfel, M. Hartwig, W. Sievers. J. Phys. Chem. Ref. Data **30**, *2*, 515 (2001). DOI: 10.1063/1.1370170
[31] G.K. White, J.G. Collins. J. Low Temper. Phys. **7**, *1*, 43 (1972). DOI: 10.1007/BF00629120
[32] T. Tsuchiya. J. Geophys. Res. **108**, *B10*, 2462 (2003). DOI: 10.1029/2003JB002446
[33] M.G. Pamato, I.G. Wood, D.P. Dobson, S.A. Hunt, L. Vočadlo. J. Appl. Crystallography **51**, *2*, 470 (2018). DOI: 10.1107/S1600576718002248
[34] P.I. Dorogokupets, T.S. Sokolova, B.S. Danilov, K.D. Litasov. Geodynamics & Tectonophysics **3**, *2*, 129 (2012). DOI: 10.5800/GT-2012-3-2-0067.
[35] C. Wong, D.E. Schuele. J. Phys. Chem. Solids **29**, *8*, 1309 (1968). DOI: 10.1016/0022-3697(68)90183-2
[36] M.N. Magomedov. Phys. Solid State **45**, *1*, 32 (2003). DOI: 10.1134/1.1537405
[37] F.D. Murnaghan. Proc. Nat. Academy Sci. USA **30**, *9*, 244 (1944). DOI: 10.1073/pnas.30.9.244
[38] S.S. Batsanov. J. Phys. Chem. Solids **124**, 327 (2019). DOI: 10.1016/j.jpcs.2018.06.002
[39] L.R. Fokin. High Temperature **58**, *2*, 173 (2020). DOI: 10.1134/S0018151X20020054
[40] L. Vitos, A.V. Ruban, H.L. Skriver, J. Kollár. Surf. Sci. **411**, *1–2*, 186 (1998). DOI: 10.1016/s0039-6028(98)00363-x
[41] Q. Jiang, H.M. Lu, M. Zhao. J. Phys.: Condens. Matter **16**, *4*, 521 (2004). DOI: 10.1088/0953-8984/16/4/001
[42] F. Aqra, A. Ayyad. Appl. Surf. Sci. **257**, *15*, 6372 (2011). DOI: 10.1016/j.apsusc.2011.01.123
[43] J. Wang, S.Q. Wang. Surf. Sci. **630**, 216 (2014). DOI: 10.1016/j.susc.2014.08.017
[44] S. Schönecker, X. Li, B. Johansson, S.K. Kwon, L. Vitos. Sci. Rep. **5**, 14860 (2015). DOI: 10.1038/srep14860
[45] R. Tran, Z. Xu, B. Radhakrishnan, D. Winston, W. Sun, K.A. Persson, S.P. Ong. Sci. Data **3**, *1*, 1−13 (2016). DOI: 10.1038/sdata.2016.80
[46] S. De Waele, K. Lejaeghere, M. Sluydts, S. Cottenier. Phys. Rev. B **94**, *23*, 235418 (2016). DOI: 10.1103/PhysRevB.94.235418
[47] T. Cheng, D. Fang, Y. Yang. Appl. Surf. Sci. **393**, 364 (2017). DOI: 10.1016/j.apsusc.2016.09.147

[48] A. Patra, J.E. Bates, J. Sun, J.P. Perdew. Proc. Nat. Academy Sci. USA **114**, *44*, E9188 (2017). DOI: 10.1073/pnas.1713320114
[49] V.P. Bokarev, G.Y. Krasnikov. Surf. Sci. **668**, 73 (2018). https://doi.org/10.1016/j.susc.2017.10.020
[50] X. Zhang, W. Li, H. Kou, J. Shao, Y. Deng, X. Zhang, J. Ma, Y. Li, X. Zhang. J. Appl. Phys. **125**, *18*, 185105 (2019). DOI: 10.1063/1.5090301
[51] M.N. Magomedov. Nanotechnolog. Russ. **14**, *1–2*, 21 (2019). DOI: 10.1134/S1995078019010063
[52] W.R. Tyson, W.A. Miller. Surf. Sci. **62**, *1*, 267 (1977). DOI: 10.1016/0039-6028(77)90442-3
[53] V.K. Kumikov, Kh.B. Khokonov. J. Appl. Phys. **54**, *3*, 1346 (1983). DOI: 10.1063/1.332209
[54] B.B. Alchagirov, T.M. Taova, Kh.B. Khokonov. Transact. of JWRI. Special Issue (Jpn) **30**, 287 (2001). https://repository.exst.jaxa.jp/dspace/handle/a-is/48071
[55] E.N. Akhmedov. J. Phys.: Conf. Ser. **1348**, 012002 (2019). DOI: 10.1088/1742-6596/1348/1/012002
[56] S.N. Zadumkin. Dokl. Akad. Nauk SSSR **112**, *3*, 453 (1957). .http://www.mathnet.ru/links/c97c74236a89a8ac731b021056fa72ca/dan21559.pdf [in Russian]
[57] M. Zhao, W. Zheng, J. Li, Z. Wen, M. Gu, C.Q. Sun. Phys. Rev. B **75**, *8*, 085427 (2007). DOI: 10.1103/PhysRevB.75.085427
[58] M.N. Magomedov. J. Surf. Investigation. X-ray, Synchrotron and Neutron Technique **6**, *1*, 86 (2012). DOI: 10.1134/S1027451012010132
[59] M.N. Magomedov. Phys. Solid State **62**, *7*, 1126 (2020). DOI: 10.1134/S1063783420070136.
[60] M.N. Magomedov. FTT **64**, *4*, 485 (2022) (in Russian). DOI: 10.21883/FTT.2022.04.52189.240

Editor T.N. Vasilevskaya